

Anomalous Roughness of Fracture Surfaces in 2D Fuse Models

Phani K.V.V. Nukala

Computer Science and Mathematics Division, Oak Ridge National Laboratory, Oak Ridge, TN 37831-6164, USA

Stefano Zapperi

*CNR-INFM, S3, Dipartimento di Fisica, Università di Modena e Reggio Emilia, Via G. Campi 213A, 41100 Modena, Italy and
ISI Foundation, Viale S. Severo 65, 10133 Torino, Italy*

Mikko J. Alava

Laboratory of Physics, Helsinki University of Technology, FIN-02015 HUT, Finland

Srđan Šimunović

Computer Science and Mathematics Division, Oak Ridge National Laboratory, Oak Ridge, TN 37831-6164, USA

We study anomalous scaling and multiscaling of two-dimensional crack profiles in the random fuse model using both periodic and open boundary conditions. Our large scale and extensively sampled numerical results reveal the importance of crack branching and coalescence of microcracks, which induce jumps in the solid-on-solid crack profiles. Removal of overhangs (jumps) in the crack profiles eliminates the multiscaling observed in earlier studies and reduces anomalous scaling. We find that the probability density distribution $p(\Delta h(\ell))$ of the height differences $\Delta h(\ell) = [h(x+\ell) - h(x)]$ of the crack profile obtained after removing the jumps in the profiles has the scaling form $p(\Delta h(\ell)) = \langle \Delta h^2(\ell) \rangle^{-1/2} f\left(\frac{\Delta h(\ell)}{\langle \Delta h^2(\ell) \rangle^{1/2}}\right)$, and follows a Gaussian distribution even for small bin sizes ℓ . The anomalous scaling can be summarized with the scaling relation $\left[\frac{\langle \Delta h^2(\ell) \rangle^{1/2}}{\langle \Delta h^2(L/2) \rangle^{1/2}}\right]^{1/\zeta_{loc}} + \frac{(\ell-L/2)^2}{(L/2)^2} = 1$, where $\langle \Delta h^2(L/2) \rangle^{1/2} \sim L^\zeta$.

I. INTRODUCTION

For over two decades, scaling of fracture surfaces has been a well studied, yet a controversial issue [1, 2]. Experiments on several materials under different loading conditions have shown that the fracture surface is self-affine [3], which implies that if the in plane length scales of a fracture surface are scaled by a factor λ then the out of plane length scales (height) of the fracture surface scales by λ^ζ , where ζ is the roughness exponent. Many experiments on several materials including metals [4], glass [5], rocks [6] and ceramics [7] have tested the scaling in three dimensions. The scaling regime in some cases has been quite impressive, spanning five decades in metallic alloys [8]. It is an interesting question as to whether the self-affinity measured so often can be replaced by more complicated scenarios and whether in any particular setup and geometry the exponents are universal as in the line-depinning scenario [9, 10].

In two dimensions, recent studies have debated the picture of simple self-affinity. In other words, for a two-dimensional crack profile $h(x)$ one can look at various statistical measures including the dependence of the roughness on sample/system size and the scaling of various moments of $h(x)$. There is a discussion on whether the two-dimensional fracture surfaces would exhibit self-affine or multi-affine scaling [11, 12, 13, 14]. Ref. [14] argues that a crack line $h(x)$ in two-dimensions is not self-affine; instead, it exhibits a much complicated multi-affine (or multiscaling) structure, with a non-constant scaling exponent ζ_q for the q -th order correlation function

$C_q(\ell) = \langle |h(x+\ell) - h(x)|^q \rangle^{1/q} \sim \ell^{\zeta_q}$. In analogy to kinetic roughening of surfaces, it has been argued that fracture surfaces exhibit anomalous scaling [15]: the *global* exponent describing the scaling of the crack width with the sample size is larger than the local exponent measured on a single sample [16, 17]. This means that the typical slope of $h(x)$ develops an algebraic dependence on the system size L , and it is necessary to introduce two roughness exponents a global one (ζ) and a local one (ζ_{loc}) whose difference measures the L -dependent extra lengthscale.

In two dimensions, the available experimental results, mainly obtained for paper samples, indicate a roughness exponent in the range $\zeta \simeq 0.6-0.7$ [11, 13, 18, 19, 20, 21]. However, one should note that apparently one can measure for various ordinary, industrial papers values that are significantly higher than $\zeta = 0.7$ [22]. The reasons for these discrepancies are not clear. It has also been noted that the roughness exponent is dependent on the crack velocity: at the onset of fast crack propagation the exponent makes a small jump from its value when the crack still grows in a stable fashion [23].

The theoretical understanding of the origin and universality of crack surface roughness is often investigated by discrete lattice (fuse, central-force, and beam) models. In these models the elastic medium is described by a network of discrete elements such as fuses, springs and beams with random failure thresholds. In the simplest approximation of a scalar displacement, one recovers the random fuse model (RFM) where a lattice of fuses with random threshold are subject to an increasing external voltage [24]. Using two-dimensional RFM, the estimated

crack surface roughness exponents are: $\zeta = 0.7 \pm 0.07$ [25], $\zeta_{loc} = 2/3$ [26], and $\zeta = 0.74 \pm 0.02$ [27]. Recently, using large system sizes (up to $L = 1024$) with extensive sample averaging, we found that the crack roughness exhibits anomalous scaling [28]. The local and global roughness exponents estimated using two different lattice topologies are: $\zeta_{loc} = 0.72 \pm 0.02$ and $\zeta = 0.84 \pm 0.03$. Anomalous scaling has been noted in the 3D numerical simulations as well [29]. The origins of anomalous scaling of fracture surfaces is not yet clear although recent studies [11, 12, 13] suggest that the origin of multiscaling and anomalous scaling in numerical simulations may be due to the existence of overhangs (jumps) in the crack profile.

In this paper, we further quantify the influence of these overhangs in the crack profiles on multi-affine scaling and anomalous scaling of crack roughness exponents. In particular, the questions we would like to address in this article are the following: (i) whether anomalous scaling of roughness observed in numerical simulations is a result of these overhangs (or jumps) in the crack profiles, and (ii) whether removing the jumps in the crack profiles completely eliminates multiscaling. This should then imply a constant scaling exponent ζ_{loc} such that the q -th order correlation function $C_q(\ell) = \langle |h(x+\ell) - h(x)|^q \rangle^{1/q} \sim \ell^{\zeta_{loc}}$. It should be noted that Gaussian distribution for $p(\Delta h(\ell))$ has been noted in Refs. [11, 12, 13, 20] only above a characteristic scale where self-affine scaling of crack surfaces is observed. In this study, we would like to further investigate whether removing these jumps in the crack profiles extends the validity of Gaussian probability density distribution $p(\Delta h(\ell))$ of the height differences $\Delta h(\ell) = [h(x+\ell) - h(x)]$ of the crack profile to even smaller window sizes ℓ . We also discuss the cases of open (OBC) and periodic boundary conditions (PBC), since the presence of the former might have an effect on whether "anomalous scaling" exists. For the PBC case, we show that the crack profiles can be collapsed to a "semi-circle law", a scaling ansatz followed by many stochastic processes that return to the origin [30]. The rest of the article consists of three sections: first we introduce the numerical details. In Section III, we go through all the numerical results, and finally Section IV presents the conclusions.

II. MODEL

We consider numerical simulations using two-dimensional random fuse model (RFM), where a lattice of fuses with random threshold are subject to an increasing external voltage [24]. The lattice system we consider is a triangular lattice of linear size L with a central notch of length a_0 (unnotched specimens imply $a_0 = 0$). All of the lattice bonds have the same conductance, but the bond breaking thresholds, t , are randomly distributed based on a thresholds probability distribution, $p(t)$. The burning of a fuse occurs irreversibly, whenever

the electrical current in the fuse exceeds the breaking threshold current value, t , of the fuse. Periodic boundary conditions are imposed in the horizontal directions (x direction) to simulate an infinite system and a constant voltage difference, V , is applied between the top and the bottom of the lattice system bus bars.

A power-law thresholds distribution $p(t)$ is used by assigning $t = X^D$, where $X \in [0, 1]$ is a uniform random variable with density $p_X(X) = 1$ and D represents a quantitative measure of disorder. The larger D is, the stronger the disorder. This results in t values between 0 and 1, with a cumulative distribution $P(t) = t^{1/D}$. The average breaking threshold is $\langle t \rangle = 1/(D+1)$, and the probability that a fuse will have breaking threshold less than the average breaking threshold $\langle t \rangle$ is $P(\langle t \rangle) = (1/(D+1))^{1/D}$. That is, the larger the D is, the smaller the average breaking threshold and the larger the probability that a randomly chosen bond will have breaking threshold smaller than the average breaking threshold.

Numerically, a unit voltage difference, $V = 1$, is set between the bus bars (in the y direction) and the Kirchhoff equations are solved to determine the current flowing in each of the fuses. Subsequently, for each fuse j , the ratio between the current i_j and the breaking threshold t_j is evaluated, and the bond j_c having the largest value, $\max_j \frac{i_j}{t_j}$, is irreversibly removed (burnt). The current is redistributed instantaneously after a fuse is burnt implying that the current relaxation in the lattice system is much faster than the breaking of a fuse. Each time a fuse is burnt, it is necessary to re-calculate the current redistribution in the lattice to determine the subsequent breaking of a bond. The process of breaking of a bond, one at a time, is repeated until the lattice system falls apart.

Using the algorithm proposed in Ref. [31], we have performed numerical simulation of fracture up to system sizes $L = 512$ for unnotched samples and up to $L = 320$ for notched samples. Our simulations cover an extensive parametric space of (L , D and a_0) given by: $L = \{64, 128, 192, 256, 320, 512\}$; $D = \{0.3, 0.4, 0.5, 0.6, 0.75, 1.0\}$; and $a_0/L = \{0, 1/32, 1/16, 3/32, 1/8, 3/16, 1/4, 5/16, 3/8\}$. A minimum of 200 realizations have been performed for each case, but for many cases 2000 realizations have been used to reduce the statistical error.

III. CRACK ROUGHNESS

A. Crack width

Once the sample has failed, we identify the final crack, which typically displays dangling ends and overhangs (see Fig. 1). We remove them and obtain a single valued crack line h_x , where the values of $x \in [0, L]$. For self-affine cracks, the local width, $w(l) \equiv \langle \sum_x (h_x -$

$(1/l) \sum_X h_X^2)^{1/2}$, where the sums are restricted to regions of length l and the average is over different realizations, scales as $w(l) \sim l^\zeta$ for $l \ll L$ and saturates to a value $W = w(L) \sim L^\zeta$ corresponding to the global width. The power spectrum $S(k) \equiv \langle \hat{h}_k \hat{h}_{-k} \rangle / L$, where $\hat{h}_k \equiv \sum_x h_x \exp i(2\pi x k / L)$, decays as $S(k) \sim k^{-(2\zeta+1)}$. When anomalous scaling is present [15, 16, 17], the exponent describing the system size dependence of the surface differs from the local exponent measured for a fixed system size L . In particular, the local width scales as $w(l) \sim l^{\zeta_{loc}} L^{\zeta - \zeta_{loc}}$, so that the global roughness W scales as L^ζ with $\zeta > \zeta_{loc}$. Consequently, the power spectrum scales as $S(k) \sim k^{-(2\zeta_{loc}+1)} L^{2(\zeta - \zeta_{loc})}$.

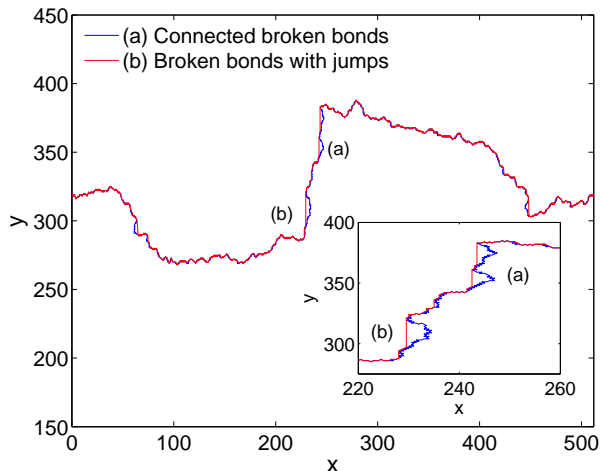


FIG. 1: (Color online) A typical crack in a fuse lattice system of size $L \times L$ with $L = 512$. This crack, identified as (a) in the figure has dangling ends, which are removed to obtain a single valued crack profile $h(x)$, identified as (b) in the figure. This final crack $h(x)$ possesses finite jumps that arise due to the solid-on-solid projection to obtain a single-valued fracture surface. The inset shows a zoomed portion of the crack.

Figure 2a presents the scaling of local and global crack widths in systems with different disorder values and an initial relative notch size of $a_0/L = 1/16$. The slopes of the curves presented in Fig. 2a suggest that a local roughness exponent $\zeta_{loc} = 0.71$ that is independent of the disorder. The global roughness exponent is estimated to be $\zeta = 0.87$, and differs considerably from the local roughness exponent ζ_{loc} . The collapse of the data in Fig. 2b clearly demonstrates that crack widths follow such an anomalous scaling law. Notice that we have scaled away the amplitudes of the roughness for all the different D to achieve the maximal data collapse to illustrate the universality. In the range of D considered here the amplitudes vary by about 20%. The inset in Fig. 2b reports the data collapse of the power spectra based on anomalous scaling for different disorder values. This collapse of the data once again suggests that local roughness is independent of disorder. A fit of the power law decay of the spectrum yields a local roughness exponent of $\zeta_{loc} = 0.74$. This result is in close agreement with the

real space estimate and we can attribute the differences to the bias associated to the methods employed [32].

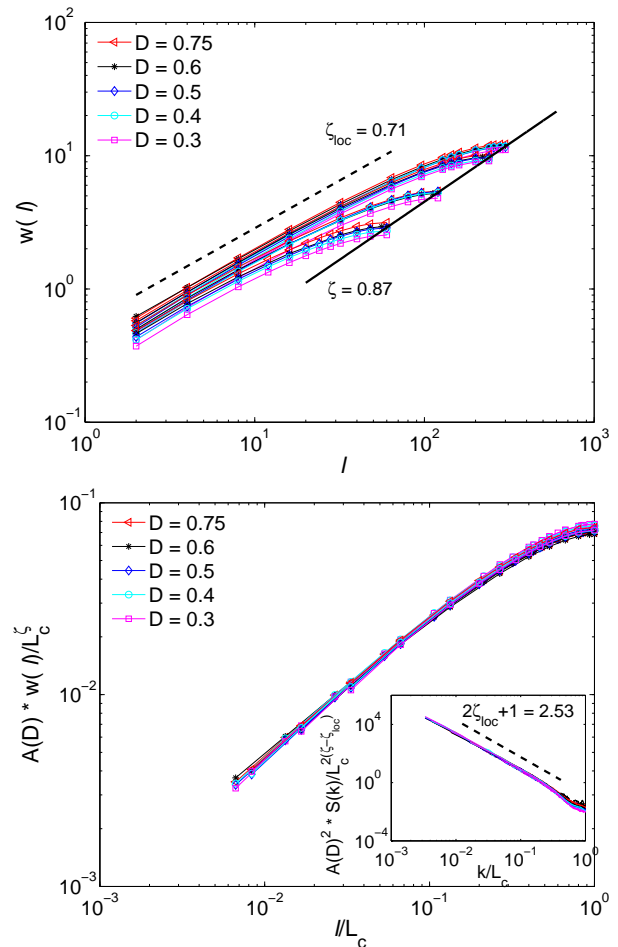


FIG. 2: (Color online) (a) Scaling of local and global widths $w(l)$ and W of the crack for different system sizes $L = \{64, 128, 256, 320\}$, disorder values D and a fixed $a_0/L = 1/16$ value (top). The local crack width exponent $\zeta_{loc} = 0.71$ is independent of disorder and differs considerably from the global crack width exponent $\zeta = 0.87$. (b) Collapse of the crack width data using the anomalous scaling law (bottom). $L_c = (L - a_0)$ is the effective length of the crack profile. Collapse of the data including a disorder dependent prefactor $A(D)$ for a given disorder value implies that local and global roughness exponents are independent of disorder. The inset shows collapse of power spectrum $S(k)$ using the anomalous scaling law with $\zeta_{loc} = 0.71$ and $\zeta = 0.87$. The slope in the inset defines the local exponent via $-(2\zeta_{loc} + 1) = -2.48$. (a)-(b) present a total of 20 data sets.

B. Anomalous Scaling

The scaling properties of the crack profiles $h(x)$ can also be studied using the probability density distribution $p(\Delta h(\ell))$ of the height differences $\Delta h(\ell) = [h(x + \ell) - h(x)]$ of the crack profile between any two points on the

reference line (x -axis) separated by a distance ℓ . Assuming the self-affine property of the crack profiles implies that the probability density distribution $p(\Delta h(\ell))$ follows the relation

$$p(\Delta h(\ell)) \sim \langle \Delta h^2(\ell) \rangle^{-1/2} f\left(\frac{\Delta h(\ell)}{\langle \Delta h^2(\ell) \rangle^{1/2}}\right) \quad (1)$$

where $\langle \Delta h^2(\ell) \rangle^{1/2}$ denotes the width of the height difference $\Delta h(\ell)$ over a length scale ℓ .

Since for PBC the periodicity in crack profiles is analogous to return-to-origin excursions arising in stochastic processes, we propose the following ansatz for the local width $\langle \Delta h^2(\ell) \rangle^{1/2}$ in height differences $\Delta h(\ell)$

$$\langle \Delta h^2(\ell) \rangle^{1/2} = \langle \Delta h^2(L/2) \rangle^{1/2} \phi\left(\frac{\ell}{L/2}\right) \quad (2)$$

with $\langle \Delta h^2(L/2) \rangle^{1/2} = L^\zeta$. The function $\phi\left(\frac{\ell}{L/2}\right)$ is symmetric about $\ell = L/2$ and is constrained such that $\phi\left(\frac{\ell}{L/2}\right) = 0$ at $\ell = 0$ and $\ell = L$, and $\phi\left(\frac{\ell}{L/2}\right) = 1$ at $\ell = L/2$. Based on these conditions, a scaling ansatz of the form

$$\left[\frac{\langle \Delta h^2(\ell) \rangle^{1/2}}{\langle \Delta h^2(L/2) \rangle^{1/2}}\right]^{1/\zeta_{loc}} + \frac{(\ell - L/2)^2}{(L/2)^2} = 1 \quad (3)$$

similar to stochastic excursions or bridges can be proposed for $\langle \Delta h^2(\ell) \rangle^{1/2}$, which implies a functional form

$$\phi\left(\frac{\ell}{L/2}\right) = \left[1 - \left(\frac{\ell - L/2}{L/2}\right)^2\right]^{\zeta_{loc}} \quad (4)$$

for $\phi\left(\frac{\ell}{L/2}\right)$ that is satisfied to a good approximation by our numerical results. This scaling ansatz implies anomalous scaling when $\zeta_{loc} \neq \zeta$. Upon further simplification, Eq. (4) results in

$$\phi\left(\frac{\ell}{L/2}\right) = 4^{\zeta_{loc}} \left(\frac{\ell}{L}\right)^{\zeta_{loc}} \left(1 - \frac{\ell}{L}\right)^{\zeta_{loc}} \quad (5)$$

which along with $\langle \Delta h^2(L/2) \rangle^{1/2} = L^\zeta$ and Eq. (2) illustrates how anomalous scaling appears in the scaling of local widths $\langle \Delta h^2(\ell) \rangle^{1/2}$, and how local and global roughness exponents ζ_{loc} and ζ can be computed based on numerical results.

Figure 3 presents the scaling of $\langle \Delta h^2(\ell) \rangle^{1/2}$ based on the above ansatz (Eq. (3)). The collapse of the $\langle \Delta h^2(\ell) \rangle^{1/2} / \langle \Delta h^2(L/2) \rangle^{1/2}$ data for different system sizes L and window sizes ℓ onto a scaling form given by Eq. (3) with $\zeta_{loc} = 0.64$ can be clearly seen in Figs. 3(a)-(c). In particular, Figs. 3(a)-(c) present the data for unnotched and notched samples with varying amounts of disorder D and relative crack sizes a_0/L . The collapse of the data for varying amounts of disorder ($0.3 \leq D \leq 1$) and relative crack sizes ($0 \leq a_0/L \leq 3/8$) can be clearly

seen in these figures and suggests that local roughness exponent ζ_{loc} is independent of disorder, at least for the disorder ranges considered here. It is an interesting question as to why the ζ_{loc} from collapsing the average crack profiles does not agree with the value from the local width, demonstrated in Fig. 2.

Figures 4(a)-(b) present the scaling of $\langle \Delta h^2(L/2) \rangle^{1/2}$ for various notched and unnotched samples with varying amounts of disorder and relative crack sizes. The data presented in these figures shows that $\langle \Delta h^2(L/2) \rangle^{1/2} \sim L^\zeta$ with $\zeta = 0.87$ in agreement with the previously given value for the global width exponent. In Figure 4(b) one can note that there is a a_0/L -dependent amplitude and the data follow the 0.87-exponent at fixed a_0/L . Since there exists a significant difference between the global and local roughness exponents (ζ and ζ_{loc} , respectively), here again we can conclude that crack profiles obtained using the fuse models exhibit anomalous roughness scaling.

The questions that we would like to resolve in the following are whether this anomalous scaling and multi-affine scaling of crack surface roughness are a consequence of the jumps in the crack profiles induced by the crack overhangs (see Fig. 1). As shown in Fig. 5, removal of jumps from an initially periodic crack profile $h(x)$ makes the resulting crack profile $h_{NP}(x)$ non-periodic, where the subscript NP refers to *nonperiodicity* of the profiles. A direct evaluation of the roughness exponent using these nonperiodic profiles can be made. However, such an evaluation of roughness exhibits finite size effects for window sizes $\ell > L/2$. Alternatively, the roughness of these resulting nonperiodic profiles can be evaluated by first subtracting a linear profile $h_{lin}(x) = \left[h_{NP}(0) + \frac{(h_{NP}(L) - h_{NP}(0))}{L}x\right]$ from the nonperiodic profile $h_{NP}(x)$, and then evaluating the roughness of the resulting periodic profile $h_P(x)$. In the following, we consider the scaling of $h_P(x)$.

Figure 6 presents the scaling of crack width $w(\ell)$ with window size ℓ for crack profiles without the jumps. The data presented in Fig. 6a suggests that local and global roughness exponents ($\zeta_{loc} = 0.74$ and $\zeta = 0.80$) are not the same even after removing the jumps in the crack profiles, although the difference between these exponents is small. We have also investigated the power spectra $S(k)$ of the crack profiles without the jumps in the crack profiles (see Fig. 6b). An excellent collapse of the data is obtained using the anomalous scaling law for power spectrum with $2(\zeta - \zeta_{loc}) = 0.1$ and $\zeta_{loc} = 0.74$. This result is consistent with the exponents measured using the crack widths as in Fig. 6a.

In addition to the above two methods (crack width scaling and power spectrum method) used for estimating the local and global roughness exponents, we also used the scaling ansatz proposed in Eq. (3) to estimate the local and global roughness exponents. Since the difference between the local and global exponents is small, alternate ways of measuring these exponents provide a sense of reliability into these estimates. Figures 7(a)-(c)

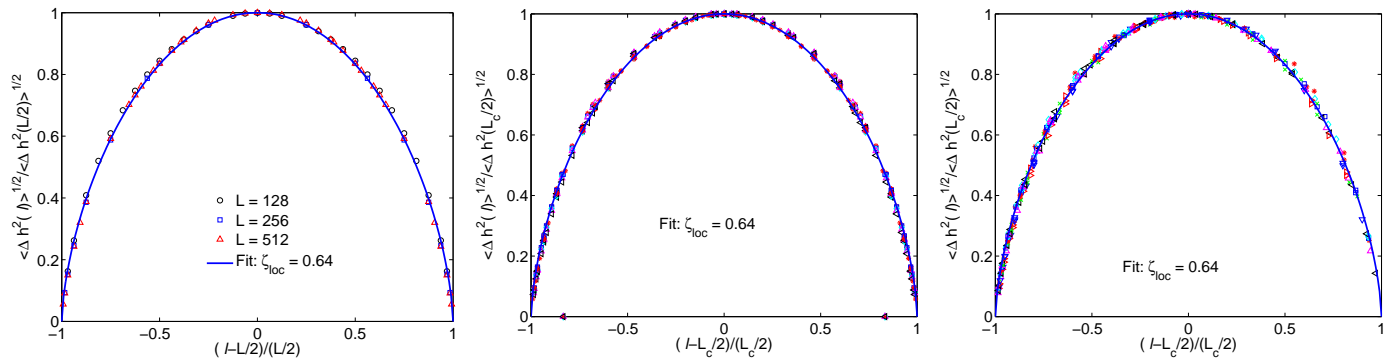


FIG. 3: (Color online) Scaling of $\langle \Delta h^2(\ell) \rangle^{1/2}$ with window size ℓ . (a) Un-notched fuse simulations for $L = \{64, 128, 256, 512\}$ and $D = 1.0$ (top left). (b) Notched fuse simulations with various disorder values $D = \{0.3, 0.4, 0.5, 0.6, 0.75\}$, system sizes $L = \{64, 128, 192, 256, 320, 512\}$, and a fixed notch size $a_0/L = 1/16$ (top middle). A total of eighteen data sets are plotted in figure. (c) Notched fuse simulations for various relative crack sizes $a_0/L = \{1/32, 2/32, 3/32, 4/32, 6/32, 8/32, 10/32, 12/32\}$, system sizes $L = \{64, 128, 256, 320\}$, and a fixed disorder of $D = 0.6$ (top right). A total of twenty four data sets are plotted in figure.

present the scaling of crack profiles $h_P(x)$. The collapse of the $\langle \Delta h_P^2(\ell) \rangle^{1/2} / \langle \Delta h_P^2(L/2) \rangle^{1/2}$ data for different system sizes L and window sizes ℓ onto a scaling form given by Eq. (3) with $\zeta_{loc} = 0.62$ can be clearly seen in Fig. 7(a). This value is fairly close to the 0.64 quoted before. In addition, the collapse of the data presented in Fig. 7(c) for $\langle \Delta h_P^q(\ell) \rangle^{1/q} / \langle \Delta h_P^q(L/2) \rangle^{1/q}$ demonstrates that multi-affine scaling of fracture surfaces arises because of overhangs (jumps) with certain statistics in the crack profile and removal of these jumps in the crack profiles completely eliminates multiscaling of fracture surfaces.

The simple scaling (no multifractality) is also evident through the scaling of $\langle \Delta h_P^q(L/2) \rangle^{1/q}$ presented in Fig. 7(b). The slopes of the data for moments $q = 1$ to 6 of $\Delta h_P(L/2)$ are identical. An interesting observation to be made is that $\langle \Delta h_P^q(L/2) \rangle^{1/q} \sim L^\zeta$ with $\zeta = 0.80$ whereas the local roughness exponent as obtained from Figs. 7(a) and (c) is $\zeta_{loc} = 0.62$. A similar behavior is observed even when the linearity in the profile is not subtracted: the scaling of these nonperiodic profiles $h_{NP}(x)$ is in agreement with that obtained for periodic profiles for window size $\ell \leq L/2$ although finite size effects are observed when window sizes $\ell > L/2$ are considered. The difference in these exponents even after removing the jumps caused by overhangs in the crack profile indicates that anomalous scaling is present in two-dimensional fracture simulations using the fuse models and this anomalous scaling is not due to the jumps in the crack profiles.

C. The case of open boundaries

It is interesting to compare the PBC case with that of open boundary conditions. Figure 8 presents the scaling of crack widths for fuse lattice simulations with open boundary conditions. The data in Fig. 8a indicates that local roughness exponent is $\zeta_{loc} = 0.75$. However, the data for different system sizes does not collapse, which

is an indication of anomalous scaling. The inset in Fig. 8a shows that a simple L-dependent shifting of the data achieves a perfect collapse of the data with possible finite size deviations for window sizes ℓ approaching the system size. Figure 8b presents the scaling of $w(\ell)$ for crack profiles without the jumps. Even after removing the jumps from the crack profiles, the crack widths data does not collapse onto a single curve. This suggests that removal of overhangs in the crack profile does not eliminate this apparent anomalous scaling of crack roughness even for open boundary conditions.

On the other hand, removing the jumps in the crack profiles once again completely eliminates the multiscaling. Figure 9a presents the scaling of q -th order correlation function $C_q(\ell) = \langle |h(x+\ell) - h(x)|^q \rangle^{1/q}$ measured using the original crack profiles. Multiscaling below a characteristic length scale can be clearly seen in Fig. 9a. The data in Fig. 9b represents the scaling of q -th order correlation function $C_q(\ell)$ measured after removing the jumps in the profiles. The Figure shows that the plots for different crack profile moments q are parallel to one another, and thus the removal of jumps in the crack profiles eliminates multiscaling. A collapse of these plots is shown in the inset and the local roughness exponent is estimated to be $\zeta_{loc} = 0.72$, close to the PBC value.

In the following, we finally investigate the probability density $p(\Delta h(\ell))$ of height differences $\Delta h(\ell)$. In Refs. [11, 13], the $p(\Delta h(\ell))$ distribution is shown to follow a Gaussian distribution above a cutoff length scale and the deviations away from Gaussian distribution in the tails of the distribution have been attributed to finite jumps in the crack profiles. A self-affine scaling of $p(\Delta h(\ell))$ as given by Eq. (1) implies that the cumulative distribution $P(\Delta h(\ell))$ scales as $P(\Delta h(\ell)) \sim P(\Delta h(\ell)) / \langle \Delta h^2(\ell) \rangle^{1/2}$. Figure 10(a) presents the raw data of cumulative probability distributions $P(\Delta h(\ell))$ of the height differences $\Delta h(\ell)$ on a normal or Gaussian paper for bin sizes $\ell \ll L$. As observed in Refs. [11, 13], and in Ref. [20] Fig. 10(a)

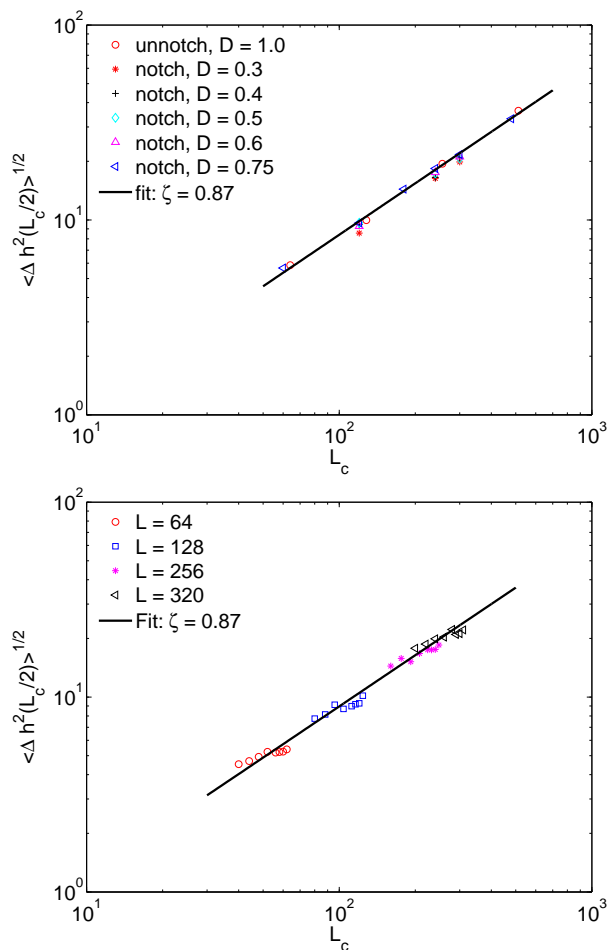


FIG. 4: (Color online) Scaling of $\langle \Delta h^2(L/2) \rangle^{1/2}$ with system size L . For notched samples, we use the effective length of the crack profile $L_c = L - a_0$. (a) Scaling of $\langle \Delta h^2(L/2) \rangle^{1/2}$ is shown for unnotched samples and for samples with a fixed relative notch size of $a_0/L = 1/16$ having varying amounts of disorder D . (b) Scaling of $\langle \Delta h^2(L_c/2) \rangle^{1/2}$ for samples with varying notch sizes and a fixed disorder of $D = 0.6$ (bottom).

shows large deviations away from Gaussian distribution for these small bin sizes. However, for moderate bin sizes, the distribution is Gaussian with deviations in the tails of the distribution beyond the $3\sigma = 3\langle \Delta h^2(\ell) \rangle^{1/2}$ limit (data not shown in Figure). Removing the jumps in the crack profiles however collapses the $P(\Delta h_P(\ell))$ distributions onto a straight line (see Fig. 10(b)) indicating the adequacy of Gaussian distribution even for small window sizes ℓ . Indeed, Fig. 10(b) shows the collapse of the $P(\Delta h_P(\ell))$ data for a system size $L = 512$ with a variety of bin sizes $2 \leq \ell \leq L/2$. Removing the jumps in the profiles not only made the $P(\Delta h_P(\ell))$ distributions Gaussian even for small window sizes ℓ but also extended the validity of $P(\Delta h_P(\ell))$ Gaussian distribution for moderate bin sizes to a $4\sigma = 4\langle \Delta h_P^2(\ell) \rangle^{1/2}$ (99.993% confidence) limit.

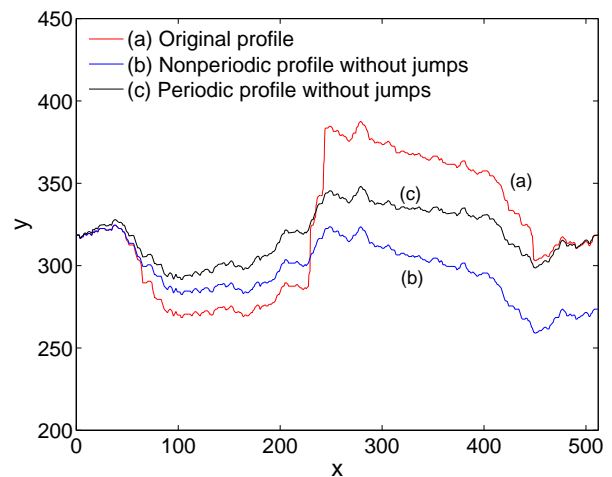


FIG. 5: (Color online) Figure shows a typical single valued crack profile $h(x)$ with jumps based on solid-on-solid projection scheme (identified as (a)). Removing the jumps in the crack profile $h(x)$ makes it a non-periodic profile (identified as (b)). Subtracting a linear profile from this non-periodic profile results in a periodic profile (identified as (c)).

IV. DISCUSSION

In summary, we have here considered the nature of the roughness of the crack surfaces in the two-dimensional RFM. The results presented here indicate universality of local roughness exponent for both notched and unnotched samples with different disorders D in the range $0.3 \leq D \leq 1.0$ and for different relative crack sizes a_0/L . This is true both for open and periodic boundary conditions.

The results indicate that anomalous scaling of roughness is a generic feature of two-dimensional fracture in the fuse model. This is in contrast to e.g. the beam model [33], where the global and local exponents are equal. The difference of the global and local exponents arises due to an additional lengthscale, which scales as a power-law of the system size L . We further investigated whether anomalous scaling of roughness is an artifact of presence of large jumps in the tails of $p(\Delta h(\ell))$ distribution. To do this, we considered the $\Delta h(\ell)$ data that is only within $\pm 3\sigma$ range of mean of $p(\Delta h(\ell))$ distribution, and computed the corresponding $\langle \Delta h^2(\ell) \rangle^{1/2}$ for various window sizes ℓ . However, the data even from these truncated $p(\Delta h(\ell))$ distributions showed anomalous scaling. We repeated our investigation with $\pm 2\sigma$ range as well, but with a similar result. This indicates that anomalous scaling of roughness is not due to the tails of $p(\Delta h(\ell))$ distribution and persists in the mean as a function of L .

Our results provide a concrete proof that the apparent multi-scaling of crack profiles observed in Ref. [14] is an artifact of jumps in the crack profiles that are formed due to the solid-on-solid approximation used in extracting the crack profiles. The removal of these jumps from the crack profiles completely eliminates this apparent multi-scaling

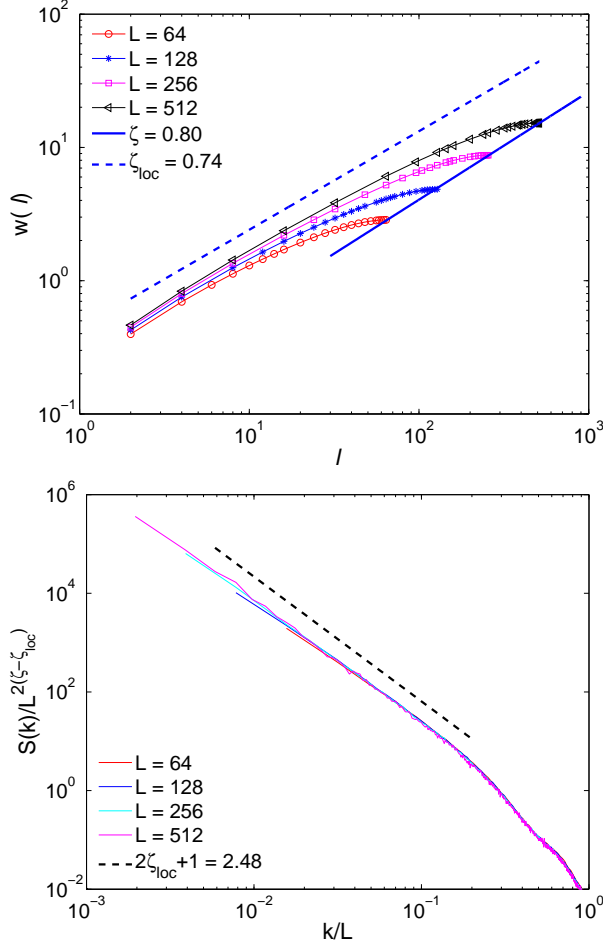


FIG. 6: (Color online) Scaling of crack profiles without the jumps. (a) Scaling of crack width $w(\ell)$. The local and global roughness exponents appear to be different although the difference is considerably smaller than that with the jumps in the profiles. (b) Scaling of power spectra of crack profiles. An excellent collapse of the data is obtained using anomalous scaling law with $2(\zeta - \zeta_{loc}) = 0.1$ and $\zeta_{loc} = 0.74$. Removal of overhangs in the crack profiles does not appear to eliminate the anomalous scaling of crack roughness in fuse models.

of crack profiles. Furthermore, removing these jumps in the crack profiles extends the validity of Gaussian probability density distribution $p(\Delta h(\ell))$ of the height differences to even smaller window sizes ℓ and to a range (of $4\sigma = 4\langle\Delta h_P^2(\ell)\rangle^{1/2}$) well beyond that observed in earlier studies.

In conclusion, though the RFM is a "toy model" of (two-dimensional here) fracture, it still poses interesting issues and can be used to study questions that are also relevant for experiments. Our numerical results presented here raise three basic theoretical questions related to the morphology of two-dimensional RFM fracture surfaces that still remain to be answered. First, why does the extra lengthscale that leads to anomalous scaling have to be algebraic? Second, models explaining the dynamics in the final avalanche (unstable crack propa-

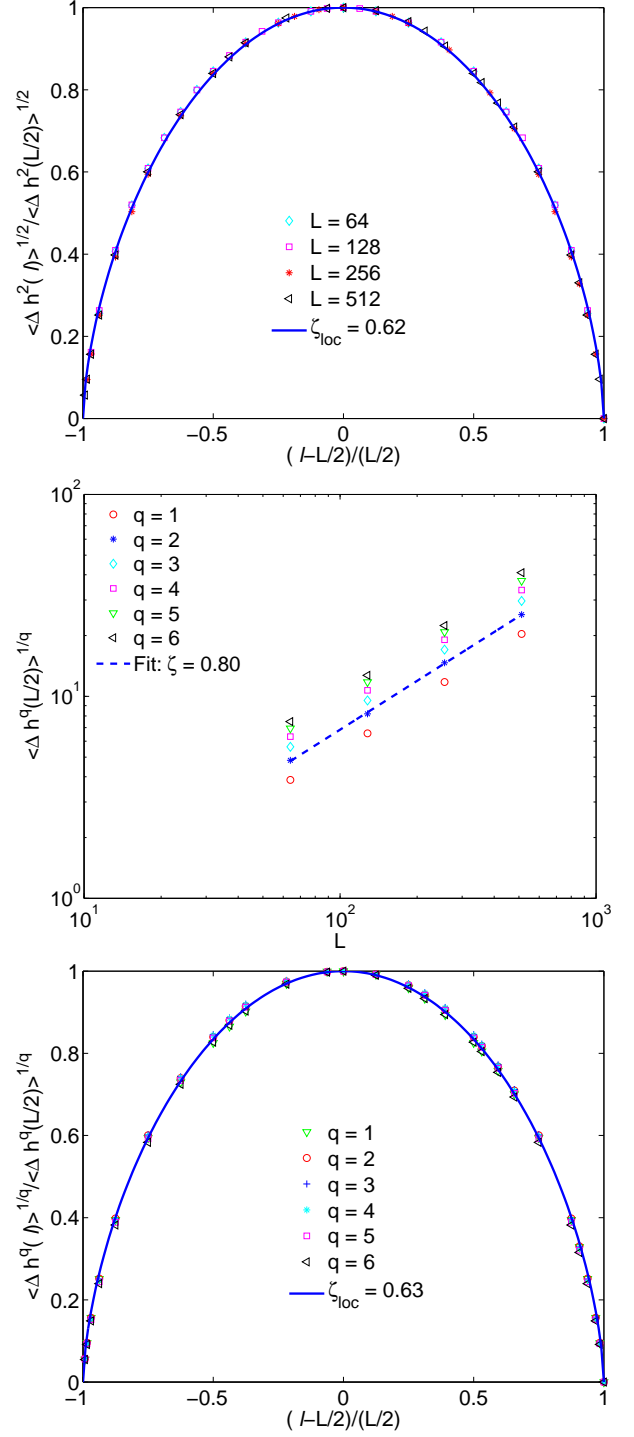


FIG. 7: (Color online) (a) Scaling of $\langle\Delta h_P^2(\ell)\rangle^{1/2}$ with window size ℓ (top); (b) Scaling of $\langle\Delta h_P^2(L/2)\rangle^{1/2}$ with system size L (middle); (c) Scaling of $\langle\Delta h_P^q(\ell)\rangle^{1/q}$ with window size ℓ for different moments q of crack profiles without overhangs (bottom).

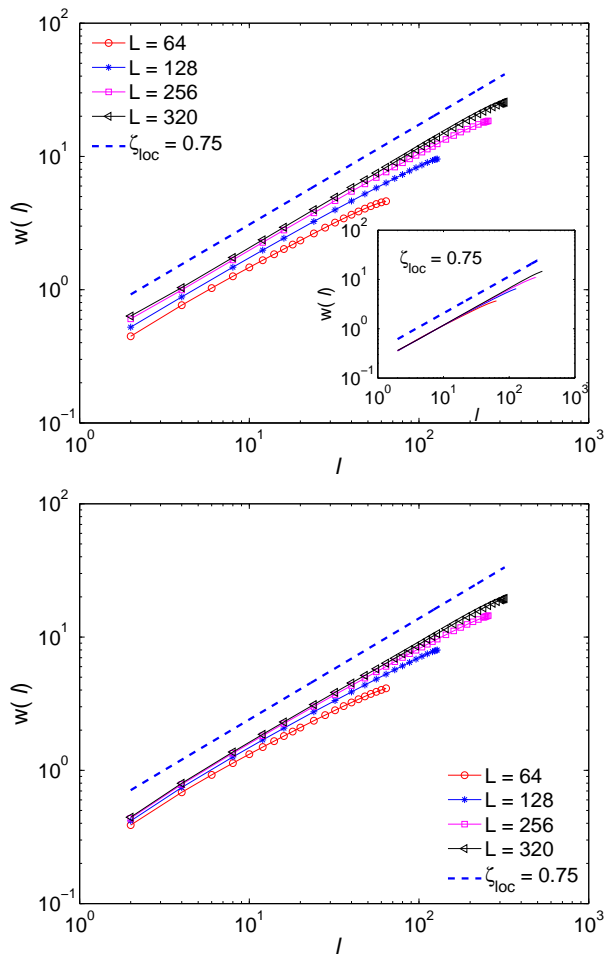


FIG. 8: (Color online) Scaling of crack width $w(\ell)$ with window size ℓ for open boundary conditions. (a) Scaling of $w(\ell)$ for crack profiles with jumps. The inset presents the data shown in the main figure after a L -dependent shift is applied. A power law fit to the data estimates the local roughness exponent to be $\zeta_{loc} = 0.75$. (b) Scaling of $w(\ell)$ for crack profiles obtained after removing the jumps. plots in figure (b) indicate that even with the removal of overhangs in the crack profile does not eliminate this apparent anomalous scaling of crack roughness.

gation) and the roughness exponent values would be theoretically interesting to develop. Third, how strong is the universality of the roughness exponents for disorders very different from the ones used here, in particular, to those leading to percolative damage or finite densities of infinitely strong fuses? Finally, in addition to presenting results that explain the origins of apparent multiscaling and anomalous scaling, we have also made a connection between periodic fracture surfaces and excursions of stochastic processes.

Acknowledgment

This research is sponsored by the Mathematical, Information and Computational Sciences Division, Office of Advanced Scientific Computing Research, U.S. Department

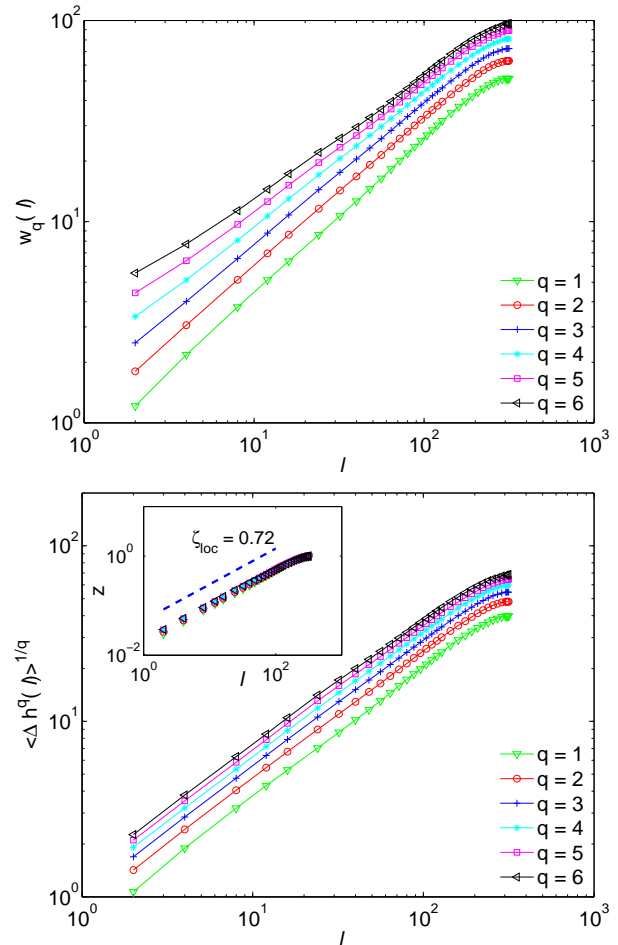


FIG. 9: (Color online) Scaling of q -th order correlation function $C_q(\ell)$. The data presented is for a system of size $L = 320$ simulated with open boundary conditions. (a) $C_q(\ell)$ measured using original crack profiles with jumps. (b) $C_q(\ell)$ measured using crack profiles without jumps. Removal of overhangs in the crack profile eliminates apparent multiscaling. Inset shows that normalization of the data leads to collapse of the curves with a local roughness exponent $\zeta_{loc} = 0.72$.

of Energy under contract number DE-AC05-00OR22725 with UT-Battelle, LLC. MJA and SZ gratefully thank the financial support of the European Commissions NEST Pathfinder programme TRIGS under contract NEST-2005-PATH-COM-043386. MJA also acknowledges the financial support from The Center of Excellence program of the Academy of Finland, and the hospitality of the Kavli Institute of Theoretical Physics, China in Beijing.

[1] H. J. Herrmann and S. Roux (eds.), *Statistical Models for the Fracture of Disordered Media*, (North-Holland, Amsterdam, 1990).

terdam, 1990).

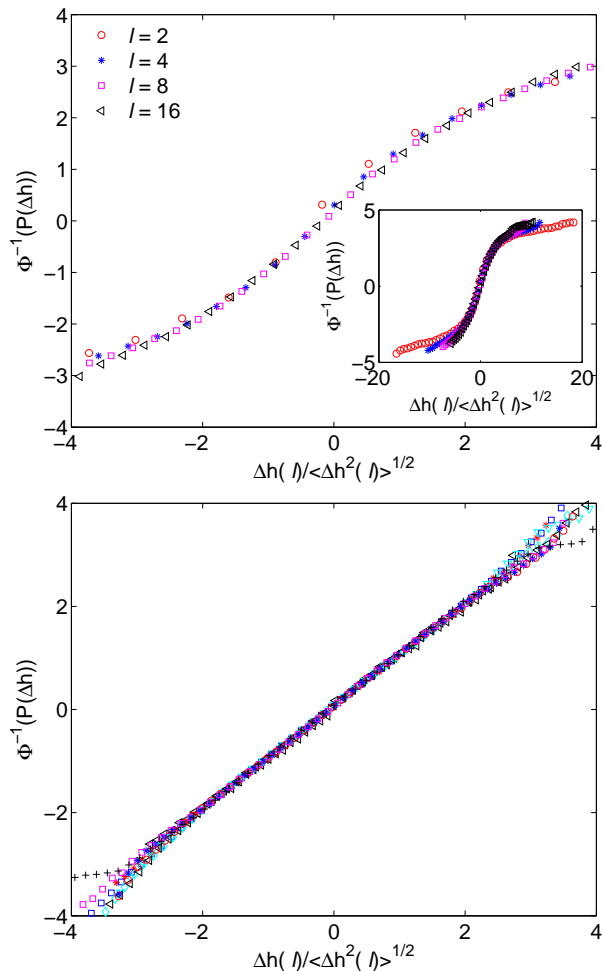


FIG. 10: (Color online) Plots of cumulative probability distributions $P(\Delta h(\ell))$ of the height differences $\Delta h(\ell) = [h(x + \ell) - h(x)]$ of the crack profile $h(x)$ for various bin sizes ℓ on a normal paper. Φ^{-1} denotes inverse Gaussian. The collapse of the profiles onto a straight line with unit slope indicates that a Gaussian distribution is adequate to represent $P(\Delta h(\ell))$. (a) $P(\Delta h(\ell))$ distributions for $L = 512$ and $\ell \ll L$. Large deviation from Gaussian profiles is observed for these window sizes. (b) Removing the jumps in the profiles however collapses the $P(\Delta h(\ell))$ distributions onto a straight line indicating the adequacy of a Gaussian even for small window sizes ℓ . The data is for $L = 512$ and $\ell = (2, 4, 8, 16, 32, 64, 96, 128, 160, 256)$.

[2] M. J. Alava, P. K. V. V. Nukala, and S. Zapperi, *Advances in Physics* **55**, 349 (2006).
 [3] B. B. Mandelbrot, D. E. Passoja, and A. J. Paullay, *Nature (London)* **308**, 721 (1984).
 [4] K.J. Maloy, A. Hansen, E.L. Hinrichsen, and S. Roux, *Phys. Rev. Lett.* **68**, 213 (1992); E. Bouchaud, G. Lapasset, J. Planés, and S. Navéos, *Phys. Rev. B* **48**, 2917 (1993).
 [5] P. Daguer, B. Nghiem, E. Bouchaud, and F. Creuzet, *Phys. Rev. Lett.* **78**, 1062 (1997).
 [6] J. Schmittbuhl, S. Roux, and Y. Berthaud, *Europhys. Lett.* **28**, 585 (1994). J. Schmittbuhl, F. Schmitt, and C.

Scholz, *J. Geophys. Res.* **100**, 5953 (1995).
 [7] J.J. Mecholsky, D.E. Passoja, and K.S. Feinberg-Ringel, *J. Am. Ceram. Soc.* **72**, 60 (1989).
 [8] For a review see E. Bouchaud, *J Phys. Condens. Matter* **9**, 4319 (1997). E. Bouchaud, *Surf. Rev. Lett.* **10**, 73 (2003).
 [9] L. Ponsou, D. Bonamy, and E. Bouchaud, *Phys. Rev. Lett.* **96**, 035506 (2006).
 [10] L. Ponsou, D. Bonamy, H. Auradou, G. Mourou, S. Morel, E. Bouchaud, C. Guillot, and J. P. Hulin, *Int. J. Fracture* **140**, 27 (2006).
 [11] M. J. Alava, P. K. V. V. Nukala, and S. Zapperi, *J. Stat. Mech.: Theor. Exp.* L10002 (2006).
 [12] J. O. H. Bakke, T. Ramstad, and A. Hansen, *Phys. Rev. B* **76**, 054110 (2007).
 [13] S. Santucci, K. J. Maloy, A. Delaplace, J. Mathiesen, A. Hansen, J. O. H. Bakke, J. Schmittbuhl, L. Vanel, and P. Ray, *Phys. Rev. E* **75**, 016104 (2007).
 [14] E. Bouchbinder, I. Procaccia, S. Santucci and L. Vanel, *Phys. Rev. Lett.* **96**, 055509 (2006) E. Bouchbinder, I. Procaccia, and S. Sela, *J. Stat. Phys.* **125**, 1029 (2006).
 [15] J. M. López, M. A. Rodríguez, and R. Cuerno, *Phys. Rev. E* **56**, 3993 (1997).
 [16] J. M. López and J. Schmittbuhl, *Phys. Rev. E* **57**, 6405 (1998).
 [17] S. Morel, J. Schmittbuhl, J. M. López, and G. Valentin, *Phys. Rev. E* **58**, 6999 (1998).
 [18] J. Kertész, V. K. Horvath, and F. Weber, *Fractals*, **1**, 67 (1993).
 [19] T. Engoy, K. J. Maloy, A. Hansen, and S. Roux, *Phys. Rev. Lett.* **73**, 834 (1994).
 [20] L. I. Salminen, M. J. Alava, and K. J. Niskanen, *Eur. Phys. J. B* **32**, 369 (2003).
 [21] J. Rosti, L. I. Salminen, E. T. Seppälä, M. J. Alava, and K. J. Niskanen, *Eur. Phys. J. B* **19**, 259 (2001).
 [22] I. L. Menezes-Sobrinho, M. S. Couto, and I. R. B. Ribeiro, *Phys. Rev. E* **71**, 066121 (2005).
 [23] N. Mallick, P.-P. Cortet, S. Santucci, S.G. Roux, L. Vanel *Phys. Rev. Lett* **98**, 255502 (2007).
 [24] L. de Arcangelis, S. Redner, and H. J. Herrmann, *J. Phys. (Paris) Lett.* **46** 585 (1985).
 [25] A. Hansen, E. L. Hinrichsen, and S. Roux, *Phys. Rev. Lett.* **66**, 2476 (1991).
 [26] E. T. Seppälä, V. I. Räsänen, and M. J. Alava *Phys. Rev. E* **61**, 6312 (2000)
 [27] J.O.H. Bakke, J. Bjelland, T. Ramstad, T. Stranden, A. Hansen, and J. Schmittbuhl, *Phys. Scripta* **T106**, 65 (2003).
 [28] S. Zapperi, P. K. V. V. Nukala, and S. Simunovic, *Phys. Rev. E* **71**, 026106 (2005).
 [29] P. K. V. V. Nukala, S. Zapperi, and S. Simunovic, *Phys. Rev. E* **74**, 026105 (2006).
 [30] A. Baldassarri, F. Colaiori, and C. Castellano, *Phys. Rev. Lett* **90**, 060601 (2003).
 [31] P. K. V. V. Nukala, and S. Simunovic, *J. Phys. A: Math. Gen.* **36**, 11403 (2003).
 [32] J. Schmittbuhl, J. P. Vilotte, and S. Roux *Phys. Rev. E* **51**, 131-147 (1995).
 [33] P. K. V. V. Nukala, S. Zapperi, M. J. Alava, S. Simunovic, preprint (2008).